



Pressure-induced amorphization in plagioclase feldspars: A time-resolved powder diffraction study during rapid compression



Melissa Sims^{a,*}, Steven J. Jaret^a, Eva-Regine Carl^b, Brandon Rhymer^a, Nadine Schrodt^c, Vivien Mohrholz^d, Jesse Smith^e, Zuzana Konopkova^f, Hanns-Peter Liermann^g, Timothy D. Glotch^a, Lars Ehm^{a,h}

^a Department of Geosciences, Stony Brook University, Stony Brook, NY 11794-2100, USA

^b Institut für Geo- und Umweltwissenschaften, Albert-Ludwig-Universität Freiburg, D-79098 Freiburg, Germany

^c Institut für Geowissenschaften, Goethe-Universität Frankfurt, D-60438 Frankfurt, Germany

^d Institut für Geowissenschaften, Friedrich-Schiller-Universität Jena, D-07737 Jena, Germany

^e High Pressure Collaborative Access Team, Carnegie Institution of Washington, Argonne, IL 60439, USA

^f European XFEL GmbH, Holzkoppel 4, 22869 Schenefeld, Germany

^g Photon Sciences, Deutsches Elektronen Synchrotron, D-22607 Hamburg, Germany

^h National Synchrotron Light Source II, Brookhaven National Laboratory, Upton, NY 11973, USA

ARTICLE INFO

Article history:

Received 3 October 2017

Received in revised form 21 November 2018

Accepted 27 November 2018

Available online 17 December 2018

Editor: W.B. McKinnon

Keywords:

plagioclase amorphization

maskelynite

rapid compression experiments

ABSTRACT

The pressure-induced amorphization of the two endmembers of the plagioclase ((Na_{1-x}Ca_x)Al_{1+x}Si_{3-x}O₈) solid-solution, anorthite (CaAl₂Si₂O₈) and albite (NaAlSi₃O₈), has been studied as a function of compression rate by means of time-resolved powder diffraction. Anorthite and albite were compressed in a diamond anvil cell to 80 GPa at multiple rates from 0.05 GPa/s to 80 GPa/s. The amorphization pressure decreases with increasing compression rate. This negative strain rate sensitivity indicates a change in deformation mechanism in the plagioclase solid-solution endmembers from brittle to ductile with increasing compression rate. The presented data support the previously proposed shear deformation mechanism for the amorphization of plagioclase. Furthermore, amorphization progresses over a wide pressure range suggesting heterogeneous amorphization, similar to observations based on recovered material from shock-compression experiments of plagioclase. Our experiments support the contention that amorphization pressures for plagioclase may occur at lower pressures than usually considered.

© 2018 Elsevier B.V. All rights reserved.

1. Introduction

Impact cratering plays an important role in the formation and evolution of planetary bodies in the Solar System (French and Short, 1968; Melosh, 1989). The continuum or peak pressure and temperature in impact materials, generally reflect impact conditions, representative of the target and impactor size, composition, and velocity (French and Short, 1968; Melosh, 1989). There is, however, considerable heterogeneity and variability in peak conditions, due to localized target properties such as porosity, grain boundary interactions, and the presence of multiple phases of different densities (Güldemeister et al., 2013; Jaret et al., 2016). In impactites at the micro-mineral scale, impact conditions can be constrained based on 1) petrographic features and 2) presence of high pressure mineral assemblages (Fritz et al., 2017; Shaw and

Walton, 2013; Stöffler, 1971, 1972, 1974; Stöffler et al., 1991; v. Engelhardt et al., 1967). Due to the abundance of feldspars in planetary crusts, amorphous plagioclase (CaAl₂Si₂O₈–NaAlSi₃O₈), known as maskelynite, is used as a key indicator for the petrographic type S5 (strongly shocked) (Stöffler, 1972, 1974; Stöffler et al., 1991; v. Engelhardt et al., 1967). Maskelynite has been found in numerous meteorites and returned samples (e.g. lunar, Martian, HEDs) and many terrestrial impactites also include maskelynite Arndt et al., 1982; Chen and El Goresy, 2000; Rubin, 2015; Stöffler et al., 1991. The presence of maskelynite indicates peak pressures between 45–55 GPa (Stöffler, 1971). Yet, the formation mechanism of maskelynite is not fully understood. Two competing formation pathways have been proposed: (1) the formation of maskelynite through quenching of a melt (Chen and El Goresy, 2000) and (2) the pressure induced transformation at high pressure and low temperature that leads to a loss of the three dimensional periodic atomic structure of plagioclase (Ashworth and Schneider, 1985; Fritz et al., 2005; Grady, 1980; Hemley et al., 1988; Jaret et al., 2015). Formation pressures for mineral phases are es-

* Corresponding author.

E-mail address: melissa.sims@stonybrook.edu (M. Sims).

timated using experimental methods, such as static diamond anvil cell (DAC), multi-anvil, and dynamic shock experiments. A number of factors affect the amorphization pressure of maskelynite, including temperature and chemical composition. Calcium content reduces the plagioclase amorphization pressure (Fritz et al., 2011; Gibbons and Ahrens, 1977). The experimental method producing amorphization also plays a role in the observed onset pressure. For maskelynite, there is a 10 GPa increase in the onset pressure for amorphization from static to dynamic techniques (Daniel et al., 1997; Ostertag, 1983; Williams and Jeanloz, 1989). This discrepancy in amorphization pressure possibly indicates a difference in transformation processes that may be inherent to the applied experimental techniques.

DAC and shock experiments differ in strain, strain rates, time scales, and temperatures compared to natural shock. Natural impacts follow the Hugoniot, with strain rates suggested to be between 10^6 – 10^9 s⁻¹ (Huffman and Reimold, 1996; Ramesh, 2008). However, impact sites may retain elevated temperatures for extended periods (Sekine, 2016). Shock experiments follow the Hugoniot (Duval and Graham, 1977; Melosh, 1989) as well, so pressures and temperatures are related to the energy of the impact. Due to differences in scale, experimental impact velocities, specific energy, and total energy are lower than those that occur in natural impact processes (Langenhorst and Hornemann, 2005). Gas-gun type shock techniques have variable strain rates, but are generally of shorter timescale than natural events (Langenhorst and Hornemann, 2005; Melosh, 1989). Due to the short timescale, some phases cannot be formed through shock experiments. Static DAC studies typically examine equilibrium states. The equilibration timescales can last up to an hour, and strain rates are low ($<10^{-2}$ s⁻¹). For reference, seismic faults have strain rates near 10^0 s⁻¹ (Spray, 2010). Experimental differences may result in discrepancies in observed formation pressures, which is problematic for phases commonly used as shock barometry indicators. If shock indicators are incorrectly calibrated, pressures determined would be incorrect, which would in turn result in errors in size estimation for impacts. A potential factor in the observed differences might be the discrepancy in compression rate between the two techniques. Changes in compression rate alter a number of mineral properties such as growth rates, morphology, defect densities, and deformation mechanisms (Lee et al., 2007). A general review of other types of strain rate experiments and the compression rates involved can be found in Ramesh (2008).

A wide range of techniques that characterize mineral structures and properties have been applied to study amorphization in plagioclase. The observed amorphization pressure varies depending on the analytical technique. Studies have used Raman spectroscopy, infrared spectroscopy, and X-ray diffraction to analyze recovered samples from static and dynamic shock experiments (Ahrens, 1964; Ahrens et al., 1969; Arndt et al., 1982; Chen and El Goresy, 2000; Daniel et al., 1997; Jaret et al., 2015; Johnson and Hörz, 2003; Johnson et al., 2003; Ostertag and Stöfler, 1982; Redfern, 1996; Tomioka et al., 2010; Velde et al., 1989; Williams, 1998; Williams and Jeanloz, 1989). In shock experiments, the transition cannot be observed *in situ*, so amorphization is determined based on analysis of recovered samples. DAC studies either used recovered samples or *in situ* techniques to determine an amorphization pressure. In DAC studies of anorthite (CaAl₂Si₂O₈), X-ray diffraction data suggests amorphization pressures higher than 16 GPa, while the same technique suggests amorphization pressures of 14–20 GPa from *in situ* work on powders (Daniel et al., 1997; Redfern, 1996). Using *in situ* infrared spectroscopy on a single crystal, amorphization pressures of 18–22 GPa were obtained (Williams and Jeanloz, 1989). Once samples were recovered, amorphization was found to be permanent only above 22 GPa as determined by Raman spectroscopy

measurements (Daniel et al., 1997). Dynamic shock experiments suggest that anorthite becomes amorphous near peak pressures of 40 GPa (Velde et al., 1989). For albite (NaAlSi₃O₈), an *in situ* infrared spectroscopy DAC study found amorphization pressures between 20–28 GPa (Williams, 1998), with an irreversible amorphization observed only in samples recovered from experiments with peak pressures greater than 24 GPa. Other shock studies on plagioclase find a transition near this pressure (Ahrens, 1964; Ahrens et al., 1973; Ahrens and Petersen, 1968; Ahrens et al., 1969; DeCarli et al., 2002, 2009; Gibbons and Ahrens, 1977). Using Raman spectroscopy on recovered powders from a DAC, Tomioka et al. (2010) reported an amorphization pressure of 39 GPa. On the other hand, Raman spectroscopy suggests that experimentally shocked albite samples require pressures above 50 GPa (Velde et al., 1989) or 50–55.8 GPa (Jaret et al., 2016) for amorphization of plagioclase.

Using a single analysis technique, the onset pressure for amorphization in static compression experiments is more than 10 GPa greater than for dynamic shock experiments (Tomioka et al., 2010). The amorphization process may demonstrate thermodynamic or mechanical differences between the two experimental types. Tomioka et al. (2010) and Langenhorst (1994) report that increasing temperature decreases amorphization pressure in pre-heated shock and static experiments. Therefore, temperature cannot be the cause of the increase in amorphization pressure since shock experiments have higher temperatures than room temperature static experiments. If the amorphization process has slow formation kinetics, time is required for the phase transition to occur and strain rate may play a role. Thus, in experiments with faster strain rates, higher amorphization pressures should be found. As suggested by previous authors, shock experiments may generally overestimate peak pressure in phases with slow kinetics (Tomioka et al., 2010).

Huffman and Reimold (1996) suggest a more fundamental amorphization mechanism where overstepping in pressure may not apply. They propose the onset pressure of the amorphization is a function of the input energy, either in the form of work done or strain rate. Hence, static compression experiments would not be able to achieve the lowest possible formation pressure due to insufficient input of work or strain energy. Furthermore, Huffman and Reimold (1996) propose that a critical ‘strain rate’ to initiate the amorphization transition may exist. This strongly suggests that the strain rates in natural impacts may produce maskelynite at lower pressures than observed in single crystal experiments. This was previously considered by Kingma et al. (1993) and Dell’Angelo (1993). Additionally, the mode of amorphization may change. Huffman and Reimold (1996) assert that high strain rates and low temperatures create more heterogeneous amorphization with optically visible planar deformations. Low strain rates and high temperatures produce more homogeneous amorphization with fine planar features. Studies of strain rate effects in feldspars can be found in Rybacki and Dresen (2004), Tullis and Yund (1987), and Tullis and Yund (1991).

Ideally, experiments should replicate a shock wave that follows the Hugoniot curve produced by the velocity of the impactor at the same timescale and compression-rate as the impactite being studied. Samples should be polycrystalline and polymineralic to account for the effect of neighboring grains. Current experimental approaches generally have substantially different conditions. In this work, we present the results of time-resolved X-ray powder diffraction experiments during fast compression of the endmembers of the plagioclase solid solution, albite and anorthite. These experiments decouple the effects of compression rate from the temperature, time, strain, and shock wave effects found in static compression and dynamic shock experiments.

2. Material and methods

Natural albite (Amelia County, Va, Sigma-Aldrich) and anorthite (Grass Valley, Ca, Ward's Science) powders were used in the experiments. Bulk samples were reduced to powder through initially grinding using a mortar and pestle followed by one hour of grinding using a McCrone micronizing mill. Grain sizes were heterogeneous prior to experimentation and had a bi-modal distribution. The average grain diameter was around 380 nm, due to the presence of many small grains. The largest grains were around 17 μm in length. Conventional X-ray powder diffraction was used to confirm the phase purity of the samples.

Symmetric DACs equipped with diamond anvils with culet diameters of 200 μm and 300 μm were used to generate pressure. The samples were placed in a hole ($\varnothing = 100 \mu\text{m}$) of a tungsten, molybdenum or steel gasket pre-indented to a thickness of about 40 μm . All experiments were conducted under non-hydrostatic conditions, without a pressure transmitting medium. The pressure was determined from the equation-of-state of an internal diffraction standard (Au (3 wt%) or NaCl (10 wt%)) mixed with the sample (Dorogokupets and Dewaele, 2007). Either a membrane (mDAC) (Letoulec et al., 1988) or piezoelectric actuator (dDAC) (Evans et al., 2007) controlled the compression rate in the experiments. We changed air pressure within the membrane to cause compression in the DAC. We could not directly control the compression rate in this type of experiment, which also do not follow the Hugoniot due to the lack of shock heating and the negligible temperature contribution from frictional forces.

We examined compression rate rather than strain rate because the strain rate is a material response to stress. We assumed strain rates of approximately 10^{-3} – 10^{-1} s^{-1} based on work by Konopkova et al. (2015). The experiment can be divided into four stages: pre-compression, compression, stabilization, and decompression. The key parameters for all experiments are summarized in Table 1. The time-resolved high-pressure diffraction experiments were conducted at the Extreme Conditions Beamline (ECB, P02.2) at PETRA III at DESY, Germany (Liermann et al., 2010) and the HPCAT beamline 16-ID-B (Shen et al., 2008) at the Advanced Photon Source at Argonne National Laboratory, USA. The diffraction images were recorded on a Perkin-Elmer (1621 CN3 EHS) flat panel detector using X-rays with a wavelength of 0.4847 \AA at the ECB at PETRA III and on a DECTRIS Pilatus 1M detector using X-rays with a wavelength of 0.6199 \AA at 16-ID-B at APS. The higher compression rates generated by the dDAC (Evans et al., 2007) required faster data collection, therefore a LAMBDA detector (X-spectrum) was used for the dDAC experiments at the ECB at PETRA III. The sample to detector distance and the geometric parameters for the radial integration of the two-dimensional diffraction data were determined from a pattern of a CeO_2 (NIST 674b) diffraction standard. The program DIOPTAS (Prescher and Prakapenka, 2015) was used to perform the conversion from diffraction images to standard one-dimensional diffraction patterns.

The lattice parameters were obtained from sequential LeBail fits to the time-resolved diffraction data employing the program TOPAS (Coelho, 2007) using a Chebyshev polynomial to describe the background and Thomson–Cox–Hastings function (Thompson et al., 1987) to model the peak profiles. The volume was calculated from the lattice parameters. Volume strain was calculated as $\Delta V/V_0$, where V is the unit cell volume and V_0 is the initial unit cell volume at ambient pressure.

We used the integrated intensities of selected diffraction maxima to follow the onset and progression of amorphization in the sample. Changes in the integrated intensity of selected peaks were used as criteria to establish the onset of amorphization. The highest value of normalized intensity was used. The disappearance of

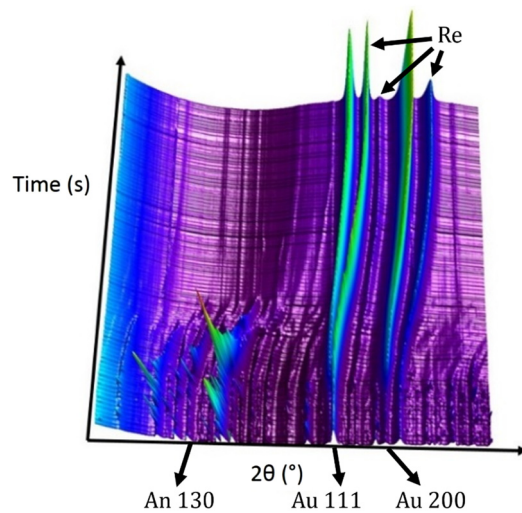


Fig. 1. 3-d plot showing the effects of ambient temperature rapid compression of anorthite consisting of a series of integrated X-ray diffraction patterns. Pressure increases with time upwards in a 0.2 GPa/s experiment. Arrows identify individual peaks from the sample (An 130), pressure standard (Au) and gasket (Re).

the Bragg peaks in the diffraction pattern marks the point of completion of the amorphization transition.

Samples recovered after decompression were studied using scanning electron microscopy (SEM). Samples were coated with gold and the examination was carried out with a Zeiss LEO 1550 field emission SEM instrument at 2.5 kV, equipped with an energy-dispersive X-ray spectrometer (EDS), at Stony Brook University.

3. Results

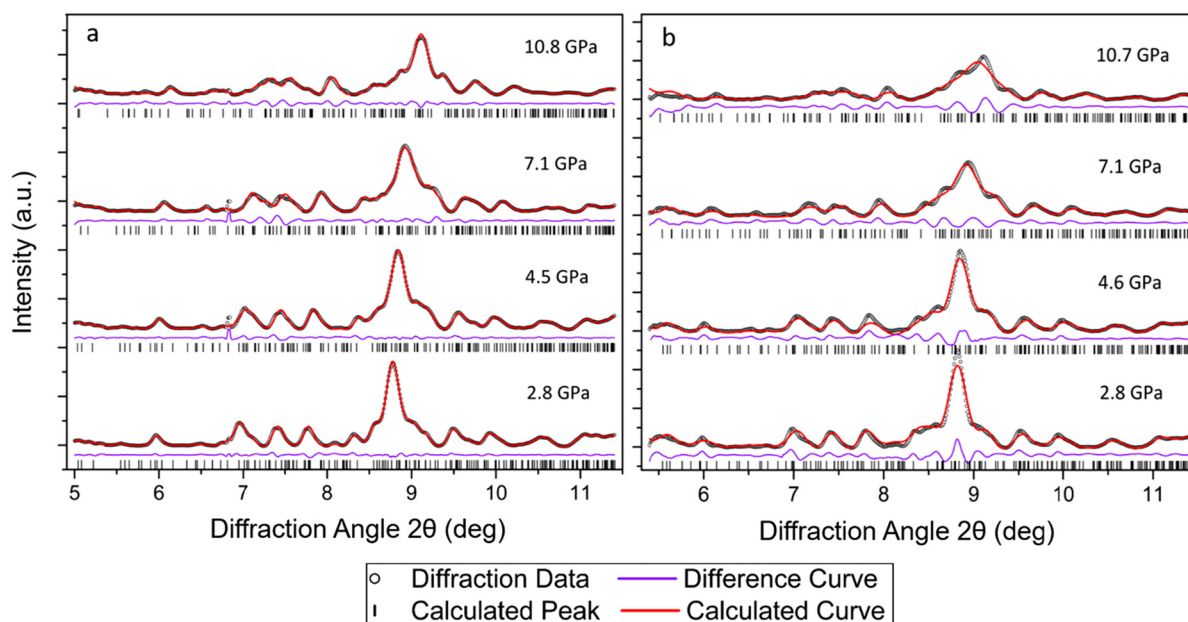
We observed amorphization at several rates for anorthite and albite samples. Fig. 1 displays a stack plot of integrated diffraction patterns from anorthite compressed at 0.2 GPa/s. It is a typical pattern for the dataset. Diffraction patterns were acquired every 1 s and were of sufficient quality for LeBail analysis (Fig. 2). Strain and size domains could not be reliably determined *in situ* due to either low intensities in the diffraction patterns or fundamental variance in sizes.

Lattice parameters were determined by performing LeBail refinement on the diffraction patterns. Fig. 3 shows plots of the unit cell volumes calculated from three compression rates for anorthite and four compression rates for albite. The initial volume for each experimental run differed, likely due to a number of variables including initial pressure and degree of amorphization of the sample. The increase in volume in the experimental run compressed at 0.8(1) GPa/s may be due to either poor LeBail fitting or differences in the elasticity of the amorphous–crystalline mix. The anorthite lattice angle β decreased slightly for the faster rates. Slower rates showed larger decreases in β (up to 3°) with increasing pressure.

For albite, the lattice parameters a , b , and c decreased for all rates with increasing pressure. The volume also decreased more sharply for faster rates. This pattern was not apparent for the anorthite data. The fit quality was sufficient for albite to use the data to calculate bulk modulus. A 2nd order Birch–Murnaghan equation was utilized, with the volume at zero pressure (V_0) set to 664.7 \AA^3 (Benusa et al., 2005) in the fit (see Table 2). Overall, increasing compression rate produced lower bulk moduli values. Therefore, albite softens with increased compression rate. The determined values were compared to static data from Benusa et al. (2005) determined from a sample from the same location. The bulk modulus from static data is higher than any found in rapidly compressed material.

Table 1
Albite and anorthite run details for all experiments.

Sample	Run #	DAC	Compression rate (GPa/s)	Peak pressure (GPa)	Holding time (s)	Exposure time (s)
Anorthite	1	mDAC	0.2(1)	62.(5)	600	1
	2	mDAC	0.3(2)	43.(5)	600	1
	3	mDAC	0.4(3)	48.(5)	600	0.5
	4	mDAC	0.6(4)	61.(5)	600	1
	5	mDAC	0.8(2)	78.(5)	600	1
	6	mDAC	0.9(1)	41.(5)	600	1
	7	dDAC	18(1)	14.(5)	1	0.1
	8	dDAC	26(0)	33.(5)	1	0.1
	9	dDAC	37(1)	44.(5)	1	0.1
Albite	1	mDAC	0.1(5)	44.(5)	600	1
	2	mDAC	0.3(3)	–	600	1
	3	mDAC	0.8(4)	51.(5)	600	1
	4	mDAC	0.9(0)	53.(5)	600	0.5
	5	mDAC	2.3(2)	23.(5)	10	1
	6	mDAC	2.6(3)	24.(5)	10	1
	7	dDAC	27(1)	26.(5)	1	0.1
	8	dDAC	35(4)	46.(5)	1	0.1
	9	dDAC	81(3)	76.(5)	1	0.1

**Fig. 2.** Two LeBail fitted plots of anorthite X-ray diffraction patterns with two different rates. a: 0.2 GPa/s b: 0.8 GPa/s. Amorphization occurs earlier in b than in a. The data is truncated prior to the gold standard peak. Black circles are data points. The red line is the calculated curve from the LeBail fit. The purple line is the difference curve between the calculated fit and data points. The black tick marks are calculated diffraction peak positions. (For interpretation of the colors in the figure(s), the reader is referred to the web version of this article.)**Table 2**

Albite 2nd order Birch–Murnaghan equation of state. Data points above 10 GPa were excluded from the fit. V_0 is initial unit cell volume, K_0 is bulk moduli, K' is the derivative of the bulk modulus.

Rate (GPa/s)	V_0 (\AA^3)	K_0 (GPa)	K'
0.1(5)	664.7	38.7(4)	4
0.3(3)	664.7	33.2(7)	4
0.8(4)	664.7	38.1(6)	4
0.9(1)	664.7	22.7(2)	4
Static ^a	664.7	52.3(9)	8.8(6)

^a Benusa et al. (2005).

A stress–volume strain plot was calculated using the albite volume data and the corresponding pressure as the stress value. We determined the slopes of the curves to produce a three-dimensional term analogous to Young's modulus. Young's modulus typically compares the change in length of the sample compared

Table 3

Albite volume strain vs stress slope calculation to 11 GPa for data from Fig. 4.

Rate (GPa/s)	Slope (GPa)
0.1(5)	44.9(7)
0.3(3)	52.8(5)
0.8(4)	47.1(3)
0.9(0)	37.2(0)

to its initial length. Due to the anisotropic compression behavior of the triclinic unit cell, volume provides a more robust measurement than individual lattice parameters.

We calculated the slopes for the stress vs. volume strain plot in Fig. 4. The stress–strain plot allows us to compare the degree of plastic deformation in samples. An increasing degree of brittleness is demonstrated by a steeper slope, while increasing ductility

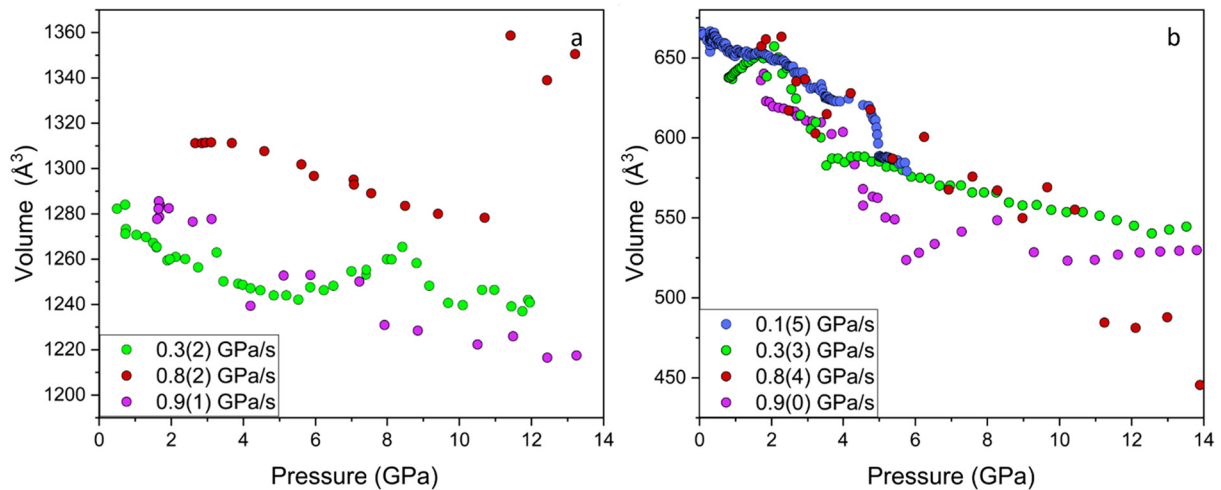


Fig. 3. Volume vs. pressure plots for a) anorthite and b) albite rapid compression experimental runs. We plot three rates in anorthite: 0.3 (green), 0.8 (red), and 0.9 GPa/s (purple); and four rates in albite: 0.2 GPa/s (blue), 0.3 GPa/s (green), 0.8 (red), and 0.9 GPa/s (purple). Error bars are small compared to the data markers. The volume data for the 0.8 GPa/s rate is likely due to problematic fitting, as the sample was predominately amorphous. Further discussion is included in the text.

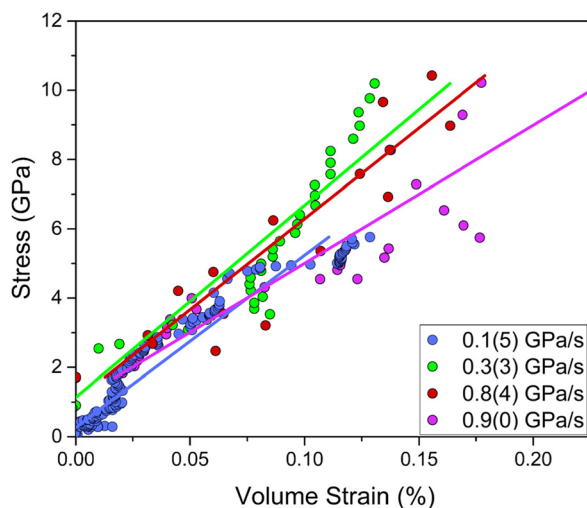


Fig. 4. Plot of the stress (experimental pressure) vs. the volume strain for albite. We plot four experimental compression rates; 0.2 GPa/s (blue), 0.3 GPa/s (green), 0.8 (red), and 0.9 GPa/s (purple). Data is truncated at 10.2 GPa. The lines are linear fits added to guide the eye. Negative volume strain points were not fit. See text for additional information.

produces shallower slopes (Byerlee, 1968). We find that with increasing compression rate, the samples become more ductile.

The amorphization point was determined using several techniques, dependent on both sample and instrumentation. The onset and completion of the amorphization was determined for all mDAC runs in anorthite (see Table 4). In anorthite mDAC experiments, three points were measured for amorphization; the onset, the disappearance of the An 130 peak, and the point at which all crystalline peaks are absent. We examined the changes in the integrated intensity of a single peak, An 130, with pressure in order to determine the onset of amorphization. Onset of amorphization behaved variably between experimental runs. The lowest onset of amorphization for anorthite mDAC experiments was found around 8 GPa for a rate of 0.56 GPa/s. The onset pressure of amorphization decreased with increasing compression rate until compression rates of 0.5–0.8 GPa/s. At higher compression rates, the onset pressure increased to between 12.4 and 13.2 GPa.

In anorthite, the completion of amorphization appeared to be relatively independent of strain rate for mDAC data. Amorphiza-

Table 4

Amorphization pressures for anorthite and albite membrane and dynamic DAC experiments. Pressures are given in GPa for An 130 onset, and complete amorphization. Rate is in GPa/s.

Type	Rate	An ₁₃₀ onset	Complete amorphization	
Anorthite	mDAC	0.2(1)	11.4(2)	32.1(1)
		0.3(2)	10.6(3)	26.6(4)
		0.4(3)	10.4(2)	24.0(4)
		0.6(4)	8.1(2)	21.2(3)
		0.8(2)	8.9(4)	30.8(1)
		0.9(1)	11.5(1)	32.9(0)
		dDAC	18(1)	–
26(0)	–		8.6(4)–12.3(3)	
37(1)	–		8.3(4)–12.0(3)	
Albite	mDAC	0.1(5)	–	31.5(4)
		0.3(3)	–	28.7(0)
		0.8(4)	–	33.3(5)
		0.9(0)	–	26.5(2)
		2.3(2)	–	17.6(1)
		2.6(3)	–	18.2(3)
		dDAC	27(1)	–
35(4)	–		22.0(1)–22.1(0)	
81(3)	–		16.5(3)–24.2(4)	

tion completion followed the trend of the disappearance of the An 130 peak. The low peak to background ratio in the dDAC experiments only allowed for the determination of the completion of the amorphization transition. For dDAC measurements, which have compression rates of several GPa per second, amorphization occurred within wide boundaries. The dDAC experiments on anorthite produced lower completion of amorphization pressures than the slower mDAC experiments. The lower bound for completion of amorphization decreases with pressure. A definite trend cannot be established due to the limited time resolution in the 26 GPa/s run.

We found that the onset pressure of amorphization generally decreases with increasing compression rate for albite mDAC data (see Fig. 5). The strong preferred orientation observed in the diffraction patterns induced during the compression of the albite sample allowed only for the unambiguous detection of the completion of the amorphization. With compression rate, there is considerable variation in completion of amorphization. The 80 GPa/s rate

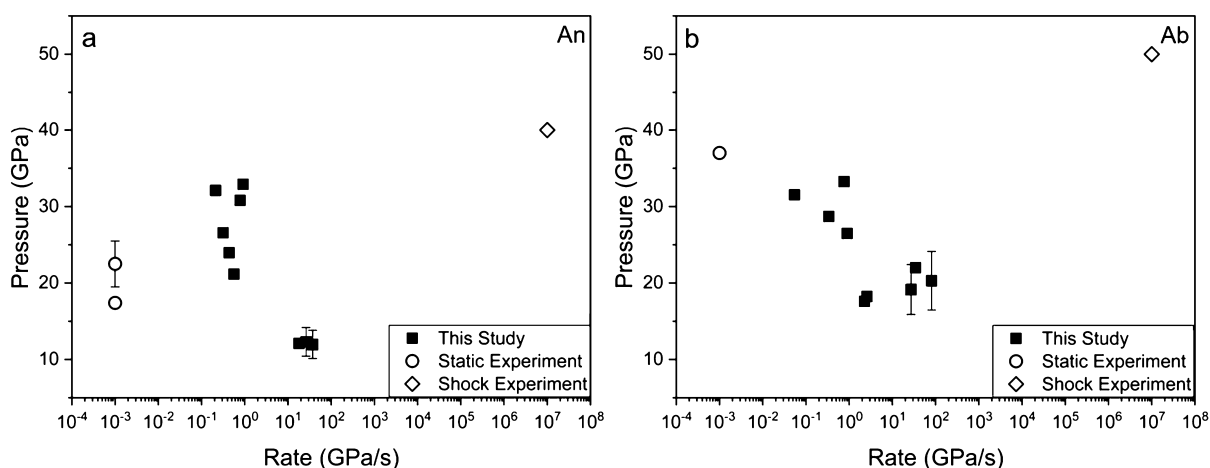


Fig. 5. a) Anorthite and b) albite total amorphization pressure vs. compression rate for all runs compared to data from previous static and shock experiments. Circles are static values (Daniel et al., 1997; Redfern, 1996; Tomioka et al., 2010), squares are from this work, diamonds are shock values (Velde et al., 1989).

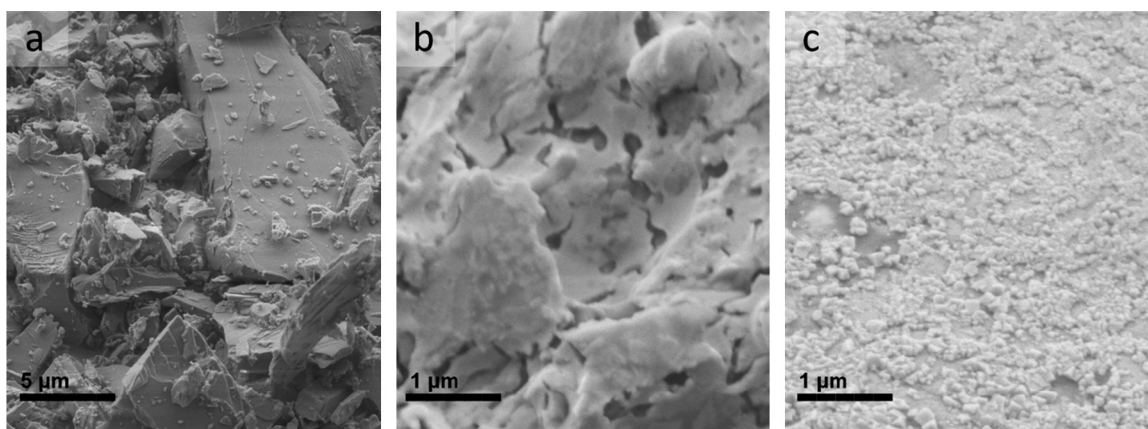


Fig. 6. SEM images of three albite samples: a) is the albite sample prior to experimentation, b) is the recovered sample from the 0.1(5) GPa/s run, and c) is the recovered sample from the 35(4) GPa/s run.

caused amorphization to end above 24.2 GPa. The ~ 2 –2.5 GPa/s runs, which were the fastest mDAC runs, produced amorphization completion pressures of 17.6(1) and 18.2(3) GPa; lower than all of the < 1 GPa/s mDAC rates. For albite, dDAC data did not suggest a similar trend as the mDAC data. The completion of the amorphization transition in the 35 GPa/s experiment was observed at 22 GPa, which is higher than completion pressures observed in ~ 2 –2.5 GPa/s mDAC data. However, to fully confirm this trend additional data at different compression rates and with higher time resolution are needed. Unfortunately, our experiments represent the current experimental limit in achievable time resolution for weakly scattering materials.

We collected SEM images of the recovered samples. The grain sizes of the recovered samples generally become finer with decreasing compression rate. The average reduced grain diameter was approximately 30 nm. The largest grains in the reduced sample were around 270 nm in diameter. Fig. 6 shows images from (a) the initial uncompressed sample, (b) a sample recovered from a 0.1(5) GPa/s run, and (c) a sample recovered from a 35(4) GPa/s run. The change in the microstructure of the recovered samples was clearly visible. The sample recovered from the slower compression rate experiment (b) showed a homogeneous distribution of sub-micron grains, while a more heterogeneous grain size and morphology was observed in (c) the sample recovered after a 35(4) GPa/s experimental run.

4. Discussion

We examine the effect of strain rate on amorphization pressure in plagioclase. We find a decrease in amorphization pressure for both anorthite and albite with increasing compression rate at strain rates around 10^{-3} s^{-1} (see Fig. 5). The observed decrease in this study seems to approach a critical transition pressure. In anorthite, amorphization completion pressure decreases to below 11 GPa or to around 8 GPa as evident from the diffraction data collected using the mDAC and dDAC, respectively. However, additional rapid compression experiments are necessary to unambiguously confirm the existence of this critical transition pressure. For albite, with increasing compression rate, amorphization pressure decreases to 17.6 GPa. If the albite dDAC diffraction data is considered, amorphization pressure possibly increases at those rates. The difference between the amorphization pressure of albite and anorthite is probably due to differences in their proposed glass structures; which require different degrees of reorientation and bond breaking (Mookherjee et al., 2016).

From our study, both the albite and anorthite samples support the Huffman and Reimold (1996) and Grady (1980) models' predictions. The amorphization pressures we observe (see Table 4) are comparable to those found in previous studies. Daniel et al. (1997) determined the onset of amorphization to be above 2 and below 9 GPa for anorthite in a quasi-hydrostatic experiment. Daniel et al.

(1997) found amorphization was complete after 11.2 GPa, which is lower than the values determined in this study. Huffman and Reimold (1996) proposed that the deformation mode changes with compression rate. High compression rates lead to heterogeneous deformation while lower compression rates should produce more homogeneous deformation in quartz and plagioclase. We observe a heterogeneous distribution of grain sizes in albite samples exposed to faster compression rates (see Fig. 6). Grain reduction occurred primarily for the largest grains. Huffman and Reimold (1996) proposed that increasing compression rate should cause the amorphization pressure to decrease until it reaches a minimum value. The grains from the slower compression rate experiments were all sub-microcrystalline, with no larger grains remaining. From our study, both the albite and anorthite samples support the model's prediction. Static experiments at arbitrary low compression rates would not produce the lowest possible amorphization pressure (Huffman et al., 1993; Huffman and Reimold, 1996). Our lowest amorphization pressure (within error bars) for anorthite of 8 GPa (Table 4) is likely not the critical transition pressure based on this model.

Our experiments may provide insight into some of the different behaviors observed in shock and static experiments that have been used to study plagioclase amorphization. If slow transformation kinetics cause the discrepancy in amorphization pressure between shock and static experiments, amorphization pressure should rise with increasing compression rate. Our experiments show that amorphization pressure does not rise with increasing compression rate, although there is some scatter (Table 4). The decrease in amorphization pressure we observe with increasing compression rate and the decrease in the bulk moduli are indicative of negative strain rate sensitivity (SRS) (van den Beukel, 1975), a plastic deformation mechanism. On the microscale, the signature for negative SRS for the semi-brittle to plastic creep deformation regime explored in our experiments is the formation of shear bands (Huffman and Reimold, 1996; van den Beukel, 1975). A change in deformation mechanism with increasing compression rate could explain the increase in amorphization pressure from our last data points to the final shock amorphization pressures from Velde et al. (1989). In addition to strain localization, additional processes, including increased plastic deformation due to elevated temperature, might increase the amorphization pressure.

The Huffman and Reimold model is based on more fundamental framework by Grady (1980) that relates strain rates and deformational modes. Grady's proposed deformation mechanism involves dissipation of elastic strain energy that produces adiabatic shear and localized 'melting'. He speculated that intrinsic instabilities in the thermomechanical deformation process in the shock regime cause deformation to be localized into thin planar regions, and the sizes of the regions are strain rate dependent. The instability should create a fundamentally chaotic appearance to data in stress-strain plots, which is observed in our data (see Fig. 4) (Evans et al., 2013; Rudnicki and Rice, 1975). The negative SRS we observe indicates formation of shear bands. Grady predicted that a reduction in strength should occur with increasing strain rate. We find evidence for this behavior in our data, where albite becomes softer and more ductile with increasing compression rate (see Table 3 and Fig. 4). Strain weakening has been observed to occur in plagioclase, although under very different conditions (Stünitz and Tullis, 2001; Svahnberg and Piazzolo, 2010).

The findings allow us to speculate about possible implications. In many materials, negative SRS only applies for a limited range of strain rates (Penning, 1972). Fig. 6 strongly suggests this might be true and that our experiments sampled the negative strain rate regime. Work hardening and grain refinement may play a role in the increase in amorphization pressure between the fastest and

slowest rapid compression runs. Grain refinement, which increases yield strength, was extreme in the 0.1 GPa/s albite run based on the SEM images (Fig. 6). The observed change amorphization onset is used here as a proxy for yield strength. Similar to our fast compression rates, shocked samples show heterogeneous deformation (Hörz and Quaide, 1973). Therefore, the type of deformation occurring in our experiments may be similar to that found in shocked systems. However, grain boundaries are typically preserved in samples recovered from shock experiments at optical scales (Hörz and Quaide, 1973; Stöffler, 1971), which we do not observe (see Fig. 6). Grady's model suggests that work hardening, which is caused by high dislocation densities, may play a role in increasing yield strength (Grady, 1980). Increasing dislocation densities then cause increases in yield strength. As dislocations pile-up, the dislocation movements cease and failure occurs. This scenario should be investigated by future studies. Poirier (1980) suggested hardening prevents strain localization, such as the formation of shear bands that plays a role in plastic deformation. This may have occurred in our slow runs, which have higher amorphization completion pressures in albite (see Table 4) and are more homogeneous (Fig. 6).

5. Conclusions

We performed *in situ* studies at various compression rates to examine deformation at atomic scales for strain rates of 10^{-3} s^{-1} . Prior research was limited to recovered samples from shock experiments. We observe a decrease in amorphization pressure with increasing compression rate. This decrease demonstrates the occurrence of negative strain rate sensitivity, which is likely caused by the motion and behavior of structural defects. Negative strain rate sensitivity implies that samples compressed at faster rates are more ductile and heterogeneous and those compressed at slower rates are more brittle and homogeneous, as was proposed by Huffman and Reimold (1996). Our data support Grady's shear deformation model (1980) for the compression rates in this study due to the more plastic and heterogeneous nature of the samples compressed at faster rates. Grady's instabilities can occur outside the shock regime. We demonstrate correlation between deformation modes and compression rates. For these reasons, amorphization in plagioclase is not likely to be an unambiguous standard to suggest specific peak pressures during shock metamorphism. We suggest amorphization pressures for plagioclase may occur at lower pressures than previously considered. We also propose that work hardening might be the mechanism responsible for producing the higher amorphization pressures seen in shock experiments.

Acknowledgements

The research was partially supported by the National Science Foundation through grant EAR-1440095 and GEO-1107155. Additional support was provided by National Aeronautics and Space Administration through the Solar System Workings program under grant 80NSSC17K0765. MS is grateful for the support of the W. Burkhardt Turner Fellowship. LE, MS, and BR acknowledge the support from the travel award by the Joint Photon Science Institute at Stony Brook University, Stony Brook, NY. TG acknowledges support from the Remote, In Situ and, and Synchrotron Studies for Science and Exploration (RIS⁴E) node of NASA's Solar System Exploration Research Virtual Institute (SSERVI). The high-pressure diffraction experiments were conducted at the Extreme Conditions Beamline (P02.2) at PETRA III at DESY and at the HPCAT beamline 16-ID-B at the Advanced Photon Source at Argonne National Laboratory. DESY is a member of the Helmholtz Association (HGF). HPCAT operations are supported by DOE-NNSA under Award No. DE-NA0001974 and DOE-BES under Award No. DE-FG02-99ER45775,

with partial instrumentation funding by NSF. The Advanced Photon Source is a U.S. Department of Energy (DOE) Office of Science User Facility operated for the DOE Office of Science by Argonne National Laboratory under Contract No. DE-AC02-06CH11357. The use of the LAMBDA detector at the Extreme Conditions Beamline (P02.2) at PETRA III at DESY was made possible by a collaborative effort by DESY and Prof. Dr. B. Winkler at Goethe University Frankfurt (Germany) supported by grant 05K13RF1 by the Federal Ministry of Education and Research (BMBF).

References

- Ahrens, T.J., 1964. Shock-metamorphism: experiments on quartz and plagioclase. In: Rosenberg, J.T. (Ed.), *Shock Metamorphism of Natural Materials*.
- Ahrens, T.J., O'Keefe, J.D., Gibbons, R.V., 1973. Shock compression of a recrystallized anorthositic rock from Apollo 15. In: *Proceedings of the Lunar Science Conference*, vol. 4, pp. 2575–2590.
- Ahrens, T.J., Petersen, C.F., 1968. Shock compression and adiabatic release of feldspars. *Trans. Am. Geophys. Union* 49, 310.
- Ahrens, T.J., Petersen, C.F., Rosenberg, J.T., 1969. Shock compression of feldspars. *J. Geophys. Res.* 74, 2727–2746.
- Arndt, J., Hummel, W., Gonzalezcabeza, I., 1982. Diaplectic labradorite glass from the manicouagan impact crater. 1. Physical-properties, crystallization, structural and genetic-implications. *Phys. Chem. Miner.* 8, 230–239.
- Ashworth, J.R., Schneider, H., 1985. Deformation and transformation in experimentally shock-loaded quartz. *Phys. Chem. Miner.* 11, 241–249.
- Benusa, M.D., Angel, R.J., Ross, N.L., 2005. Compression of albite, NaAlSi₃O₈. *Am. Mineral.* 90, 1115–1120.
- Chen, M., El Goresy, A., 2000. The nature of maskelynite in shocked meteorites: not diaplectic glass but a glass quenched from shock-induced dense melt at high pressures. *Earth Planet. Sci. Lett.* 179, 489–502.
- Coelho, A., 2007. TOPAS Academic: General Profile and Structure Analysis Software for Powder Diffraction Data. Bruker AXS, Karlsruhe, Germany.
- Byerlee, J.D., 1968. Brittle–ductile transition in rocks. *J. Geophys. Res.* 73, 4741–4750.
- Daniel, I., Gillet, P., McMillan, P.F., Wolf, G., Verhelst, M.A., 1997. High-pressure behavior of anorthite: compression and amorphization. *J. Geophys. Res., Solid Earth* 102, 10313–10325.
- DeCarli, P.S., Bowden, E., Jones, A.P., Price, G.D., 2002. Laboratory impact experiments versus natural impact events. In: *Catastrophic Events and Mass Extinctions: Impacts and Beyond*, vol. 356, pp. 595–605.
- DeCarli, P.S., Xie, Z.D., Sharp, T.G., 2009. Discrepancies between laboratory shock experiments on minerals and natural events. In: *American Geophysical Union Fall Meeting*. #MR12A-07.
- Dell'Angelo, L., 1993. Defect structures in a quartz-tremolite rock under high stresses: evidence for amorphization. In: McLaren, A.C., Boland, J.N., Fitz Gerald, J.D. (Eds.), *Defects and Processes in the Solid State: Geoscience Applications: the McLaren Volume*. Elsevier, Amsterdam.
- Dorogokupets, P.I., Dewaele, A., 2007. Equations of state of MgO, Au, Pt, NaCl-B1, and NaCl-B2: internally consistent high-temperature pressure scales. *High Press. Res.* 27, 431–446.
- Duval, G.E., Graham, R.A., 1977. Phase-transitions under shock-wave loading. *Rev. Mod. Phys.* 49, 523–579.
- Evans, B., Fredrich, J.T., Wong, T., 2013. The brittle–ductile transition in rocks: recent experimental and theoretical progress. In: *The Brittle–Ductile Transition in Rocks*. American Geophysical Union, pp. 1–20.
- Evans, W.J., Yoo, C.S., Lee, G.W., Cynn, H., Lipp, M.J., Visbeck, K., 2007. Dynamic diamond anvil cell (dDAC): a novel device for studying the dynamic-pressure properties of materials. *Rev. Sci. Instrum.* 78, 073904.
- French, B.M., Short, N.M., 1968. *Shock Metamorphism of Natural Materials*. Mono Book Corporation, Baltimore.
- Fritz, J., Greshake, A., Fernandes, V.A., 2017. Revising the shock classification of meteorites. *Meteorit. Planet. Sci.* 52, 1216–1232. <https://doi.org/10.1111/maps.12845>.
- Fritz, J., Greshake, A., Stöffler, D., 2005. Micro-Raman spectroscopy of plagioclase and maskelynite in Martian meteorites: evidence of progressive shock metamorphism. *Antarct. Meteor. Res.* 18, 96.
- Fritz, J., Wuenemann, K., Greshake, A., Fernandes, V., Boettger, U., Hornemann, U., 2011. Shock pressure calibration for lunar plagioclase. In: *Lunar and Planetary Science Conference XLII*.
- Gibbons, R.V., Ahrens, T.J., 1977. Effects of shock pressure on calcic plagioclase. *Phys. Chem. Miner.* 1, 95–107.
- Grady, D., 1980. Shock deformation of brittle solids. *J. Geophys. Res., Solid Earth* 85, 913–924.
- Güldemeister, N., Wünnemann, K., Durr, N., Hiermaier, S., 2013. Propagation of impact-induced shock waves in porous sandstone using mesoscale modeling. *Meteorit. Planet. Sci.* 48, 115–133.
- Hemley, R.J., Jephcoat, A.P., Mao, H.K., Ming, L.C., Manghni, M.H., 1988. Pressure-induced amorphization of crystalline silica. *Nature* 334, 52–54.
- Hörz, F., Quaide, W., 1973. Debye–Scherrer investigations of experimentally shocked silicates. *Moon* 6, 45–82.
- Huffman, A.R., Brown, J.M., Carter, N.L., Reimold, W.U., 1993. The microstructural response of quartz and feldspar under shock loading at variable temperatures. *J. Geophys. Res., Solid Earth* 98, 22171–22197.
- Huffman, A.R., Reimold, W.U., 1996. Experimental constraints on shock-induced microstructures in naturally deformed silicates. *Tectonophysics* 256, 165–217.
- Jaret, S.J., Johnson, J.R., Sims, M., Glotch, T.D., 2016. Micro-Raman spectroscopy of experimentally shocked albite. In: *Lunar and Planetary Science Conference XLVII*.
- Jaret, S.J., Woerner, W.R., Phillips, B.L., Ehm, L., Nekvasil, H., Wright, S.P., Glotch, T.D., 2015. Maskelynite formation via solid–state transformation: evidence of infrared and X-ray anisotropy. *J. Geophys. Res., Planets* 120, 570–587.
- Johnson, J.R., Horz, F., Staid, M.I., 2003. Thermal infrared spectroscopy and modeling of experimentally shocked plagioclase feldspars. *Am. Mineral.* 88, 1575–1582.
- Johnson, J.R., Hörz, F., 2003. Visible/near-infrared spectra of experimentally shocked plagioclase feldspars. *J. Geophys. Res., Planets* 108, 5120.
- Kingma, K.J., Meade, C., Hemley, R.J., Mao, H.-k., Veblen, D.R., 1993. Microstructural observations of α -quartz amorphization. *Science* 259, 666–669.
- Langenhorst, F., 1994. Shock experiments on pre-heated α - and β -quartz: II. X-ray and TEM investigations. *Earth Planet. Sci. Lett.* 128, 683–698. [https://doi.org/10.1016/0012-821X\(94\)90179-1](https://doi.org/10.1016/0012-821X(94)90179-1).
- Langenhorst, F., Hornemann, U., 2005. Shock experiments on minerals: basic physics and techniques. In: *EMU Notes in Mineralogy*, vol. 7, pp. 357–387.
- Lee, G.W., Evans, W.J., Yoo, C.S., 2007. Dynamic pressure-induced dendritic and shock crystal growth of ice VI. *Proc. Natl. Acad. Sci. USA* 104, 9178–9181.
- Letoulliec, R., Pinceaux, J.P., Loubeyre, P., 1988. The membrane diamond anvil cell: a new device for generating continuous pressure and temperature variations. *High Press. Res.* 1, 77–90.
- Liermann, H.P., Morgenroth, W., Ehnes, A., Berghäuser, A., Winkler, B., Franz, H., Weckert, E., 2010. The extreme conditions beamline at PETRA III, DESY: possibilities to conduct time resolved monochromatic diffraction experiments in dynamic and laser heated DAC. *J. Phys. Conf. Ser.* 215, 012029.
- Melosh, J., 1989. *Impact Cratering: A Geologic Process*. Oxford University Press, New York.
- Mookherjee, M., Mainprice, D., Maheshwari, K., Heinonen, O., Patel, D., Hariharan, A., 2016. Pressure induced elastic softening in framework aluminosilicate-albite (NaAlSi₃O₈). *Sci. Rep.* 6, 34815.
- Ostertag, R., 1983. Shock experiments on feldspar crystals. *J. Geophys. Res., Solid Earth* 88, B364–B376.
- Ostertag, R., Stöffler, D., 1982. Thermal annealing of experimentally shocked feldspar crystals. *J. Geophys. Res.* 87, A457–A463.
- Penning, P., 1972. Mathematics of Portevin–Le Chatelier effect. *Acta Metall.* 20 (10), 1169.
- Poirier, J.P., 1980. Shear localization and shear instability in materials in the ductile field. *J. Struct. Geol.* 2, 135–142.
- Prescher, C., Prakupenka, V.B., 2015. DIOPTAS: a program for reduction of two-dimensional X-ray diffraction data and data exploration. *High Press. Res.* 35, 223–230.
- Ramesh, K.T., 2008. High rates and impact experiments. In: Sharp, W.N. (Ed.), *Springer Handbook of Experimental Solid Mechanics*. Springer, Boston.
- Redfern, S.A.T., 1996. Length scale dependence of high-pressure amorphization: the static amorphization of anorthite. *Mineral. Mag.* 60, 493–498.
- Rubin, A.E., 2015. Maskelynite in asteroidal, lunar and planetary basaltic meteorites: an indicator of shock pressure during impact ejection from their parent bodies. *Icarus* 257, 221–229.
- Rudnicki, J.W., Rice, J.R., 1975. Conditions for the localization of deformation in pressure-sensitive dilatant materials. *J. Mech. Phys. Solids* 23, 371–394.
- Rybacki, E., Dresen, D., 2004. Deformation mechanism maps for feldspar rocks. *Tectonophysics* 382, 173–187.
- Sekine, T., 2016. Problems in comparison between natural and experimental shocks. In: *79th Annual Meeting of the Meteoritical Society*.
- Shaw, C.S., Walton, E., 2013. Thermal modeling of shock melts in Martian meteorites: implications for preserving Martian atmospheric signatures and crystallization of high-pressure minerals from shock melts. *Meteorit. Planet. Sci.* 48, 758–770. <https://doi.org/10.1111/maps.12100>.
- Shen, G., Chow, P., Xiao, Y., Sinogeikin, S., Meng, Y., Yang, W., Liermann, H.-P., Shebanova, O., Rod, E., Bommannavar, A., Mao, H.-K., 2008. HPCAT: an integrated high-pressure synchrotron facility at the advanced photon source. *High Press. Res.* 28, 145–162.
- Spray, J.G., 2010. Frictional melting processes in planetary materials: from hypervelocity impact to earthquakes. *Annu. Rev. Earth Planet. Sci.* 38, 221–254.
- Stöffler, D., 1971. Progressive metamorphism and classification of shocked and brecciated crystalline rocks at impact craters. *J. Geophys. Res.* 76, 5541–5551.
- Stöffler, D., 1972. Deformation and transformation of rock-forming minerals by natural and experimental shock processes. I – Behavior of minerals under shock compression. *Fortschr. Mineral.* 49, 64.
- Stöffler, D., 1974. Deformation and transformation of rock-forming minerals by natural and experimental shock processes. II. *Fortschr. Mineral.* 51, 256–289.
- Stöffler, D., Keil, K., Scott, E.R.D., 1991. Shock metamorphism of ordinary chondrites. *Geochim. Cosmochim. Acta* 55, 3845–3867.

- Stünitz, H., Tullis, J., 2001. Weakening and strain localization produced by syn-deformational reaction of plagioclase. *Int. J. Earth Sci.* 90, 136–148.
- Svahnberg, H., Piazzolo, S., 2010. The initiation of strain localisation in plagioclase-rich rocks: insights from detailed microstructural analyses. *J. Struct. Geol.* 32, 1404–1416.
- Thompson, P., Cox, D.E., Hastings, J.B., 1987. Rietveld refinement of Debye–Scherrer synchrotron X-ray data from Al₂O₃. *J. Appl. Crystallogr.* 20, 79–83.
- Tomioka, N., Kondo, H., Kunikata, A., Nagai, T., 2010. Pressure-induced amorphization of albitic plagioclase in an externally heated diamond anvil cell. *Geophys. Res. Lett.* 37, L21301.
- Tullis, J., Yund, R.A., 1987. Transition from cataclastic flow to dislocation creep of feldspar: mechanisms and microstructures. *Geology* 15, 606–609.
- Tullis, J., Yund, R.A., 1991. Diffusion creep in feldspar aggregates: experimental evidence. *J. Struct. Geol.* 13, 987–1000.
- v. Engelhardt, W., Bertsch, W., Stöffler, D., Groschopf, P., Reiff, W., 1967. Anzeichen für den meteoritischen Ursprung des Beckens von Steinheim. *Naturwissenschaften* 54, 198–199.
- van den Beukel, A., 1975. Theory of the effect of dynamic strain aging on mechanical properties. *Phys. Status Solidi A* 30, 197–206.
- Velde, B., Syono, Y., Kikuchi, M., Boyer, H., 1989. Raman microprobe study of synthetic diaplectic plagioclase feldspars. *Phys. Chem. Miner.* 16, 436–441.
- Williams, Q., 1998. High-pressure infrared spectra of feldspars: constraints on compressional behavior, amorphization, and diaplectic glass formation. In: *Properties of Earth and Planetary Materials at High Pressure and Temperature*, vol. 101, pp. 531–543.
- Williams, Q., Jeanloz, R., 1989. Static amorphization of anorthite at 300-K and comparison with diaplectic glass. *Nature* 338, 413–415.